




Article

Detection of Growth Change of Young Forest Based on UAV RGB Images at Single-Tree Level

Xiaocheng Zhou ^{1,*}, Hongyu Wang ¹, Chongcheng Chen ¹, Gábor Nagy ², Tamas Jancso ²
and Hongyu Huang ¹

¹ Key Laboratory of Spatial Data Mining and Information Sharing of Ministry of Education, National & Local Joint Engineering Research Center of Satellite Geospatial Information Technology, Fuzhou University, Fuzhou 350108, China

² Institute of Geoinformatics, Alba Regia Technical Faculty, Obuda University, 8000 Székesfehérvár, Hungary

* Correspondence: zhouxc@fzu.edu.cn; Tel.: +86-0591-63179578

Abstract: With the rapid development of Unmanned Aerial Vehicle (UAV) technology, more and more UAVs have been used in forest survey. UAV (RGB) images are the most widely used UAV data source in forest resource management. However, there is some uncertainty as to the reliability of these data when monitoring height and growth changes of low-growing saplings in an afforestation plot via UAV RGB images. This study focuses on an artificial Chinese fir (*Cunninghamia lanceolata*, named as Chinese Fir) young forest plot in Fujian, China. Divide-and-conquer (DAC) and the local maximum (LM) method for extracting seedling height are described in the paper, and the possibility of monitoring young forest growth based on low-cost UAV remote sensing images was explored. Two key algorithms were adopted and compared to extract the tree height and how it affects the young forest at single-tree level from multi-temporal UAV RGB images from 2019 to 2021. Compared to field survey data, the R^2 of single saplings' height extracted from digital orthophoto map (DOM) images of tree pits and original DSM information using a divide-and-conquer method reached 0.8577 in 2020 and 0.9968 in 2021, respectively. The RMSE reached 0.2141 in 2020 and 0.1609 in 2021. The R^2 of tree height extracted from the canopy height model (CHM) via the LM method was 0.9462. The RMSE was 0.3354 in 2021. The results demonstrated that the survival rates of the young forest in the second year and the third year were 99.9% and 85.6%, respectively. This study shows that UAV RGB images can obtain the height of low sapling trees through a computer algorithm based on using 3D point cloud data derived from high-precision UAV images and can monitor the growth of individual trees combined with multi-stage UAV RGB images after afforestation. This research provides a fully automated method for evaluating the afforestation results provided by UAV RGB images. In the future, the universality of the method should be evaluated in more afforestation plots featuring different tree species and terrain.

Keywords: unmanned aerial vehicle; forest survey; saplings; tree height; height change; RGB images



Citation: Zhou, X.; Wang, H.; Chen, C.; Nagy, G.; Jancso, T.; Huang, H. Detection of Growth Change of Young Forest Based on UAV RGB Images at Single-Tree Level. *Forests* **2023**, *14*, 141. <https://doi.org/10.3390/f14010141>

Academic Editor: Gherardo Chirici

Received: 22 November 2022

Revised: 2 January 2023

Accepted: 10 January 2023

Published: 12 January 2023



Copyright: © 2023 by the authors. Licensee MDPI, Basel, Switzerland. This article is an open access article distributed under the terms and conditions of the Creative Commons Attribution (CC BY) license (<https://creativecommons.org/licenses/by/4.0/>).

1. Introduction

Forest inventory is a basic technical method used to obtain forest resource information and make various forestry analyses and decisions [1]. In a forest inventory, tree height, crown and diameter at breast height (DBH) information are of the most important forest parameters. In general, manual measurement forest parameters is inefficient and time consuming [2–4]. Studies have demonstrated that a wide range of forest parameter information can be quickly obtained with high accuracy through UAV remote sensing. For example, information such as tree height, tree number, and tree crown can be quickly obtained via UAV remote sensing [5–8]. In addition, the accurate acquisition of forest parameter information is of great significance for future forest management.

Tree height is a critical parameter in forest resource inventory and is usually used as an indicator of forest growth, biomass and forest health evaluation [9,10]. The tree

height measurement method directly or indirectly measures the distance between the base (ground) and the top (apical meristem) of a tree in the field. The traditional measurement method uses a telescopic measuring rod to measure the tree height directly or uses cut down trees and measures the tree length with a tape. In addition, some workers estimate the height of trees with their eyes or use a total station to measure the height of each tree. These methods of measurement at the single tree level are expensive and time consuming and are generally unsuitable for large region surveys. However, an indirect measure of a single tree via digital UAV photogrammetry is a good alternative [11,12]. Some scholars discussed the possibility of using UAV remote-sensing technology to expand the scope of a forest survey and potentially replace the traditional forest survey altogether [13]. Most tree parameters are closely related to tree height, and tree attribute estimation requires tree height as an input parameter [14]. Over the last decade, the forest resource survey based on remote sensing has made significant progress. High-precision UAV remote-sensing images and image processing algorithms were used to estimate forest land with centimeter resolution [15,16]. In the past, many studies have used UAV data to build canopy height models to estimate tree height [17–19]. This method provides good accuracy for tree height obtained in flat woodland [20]. However, the method may lead to errors in forest plots with high canopy closure and large slopes [21,22].

Most UAV remote sensing research has focused on surveys of middle and mature forests, and few authors have reported applications of UAV remote sensing in young forests [23–25]. These studies demonstrate that high-precision tree-height information can be obtained by the local maximum (LM) method. The advantage of this method is that it has higher accuracy in the higher trees. However, for the young trees with small size and blurred canopies and varying sizes, it is difficult for the LM algorithm to determine the location of trees, and there is a large error in height estimation. In addition, some scholars [26] tried to use RGB images from UAV to detect fir forest seedlings, but the detection accuracy was limited (detection rate = 75.8%, $n = 149$). Hartley [27] found a high correlation ($R^2 > 0.9$) between the predicted tree height and the measured tree height of young stands below 1 m in a forestry experiment in the central North Island of New Zealand, but there is a large relative error between the measured value and the estimated value. Earlier studies have demonstrated that the young trees similar to the stump can be detected from UAV images via an automatic or semi-automatic method [28,29]. In conclusion, it is of great significance to evaluate young forest parameters through UAV image assessment and monitoring.

A survival rate indicator for artificial saplings can be used to evaluate the tree growth status and environmental changes. It can be calculated by tree height change in the second year. Researchers usually measured individual trees at certain time intervals. The sample trees in many forest plots are measured and observed for many years and the height change of the trees is evaluated [30]. However, UAV images have not been used for the accurate assessment and long-term growth monitoring of young forests at single tree level. The purpose of this paper was to evaluate the feasibility of estimating the height and annual growth of young forests after afforestation based on annual optical UAV remote sensing. We aimed to use the 3D point cloud data from UAV RGB images to extract the tree height of young forests, and their height changes over the years at the single tree level.

2. Data

2.1. Study Region

The study region is located in Jiangle County, Fujian Province, China (26.728953° N, 117.471373° E). The climate is a subtropical monsoon climate, and the average rainfall was 2701.4 mm in 2021. The Jiangle county is very rich in forest resources. The total area of the county is 192,000 ha, of which the forest coverage rate accounts for 85.2%. The study region is located at a young Chinese fir forest plot in Jiangle County, with a size of 4300 m² of young forest on a slope of up to or approximately 24 degrees (Figure 1). The forest of the study region was deforested in 2018, then artificial afforestation began in January

2019. Saplings of 30 cm–45 cm in length were planted in May 2019. The height of the seedlings above the ground was about 10 cm. In our field survey, the study area did not receive disruptive changes between 2019 and 2020. In 2021, artificial structures and a stone road were constructed in the study area. In addition, we conducted field surveys and data collection and found changes in tree species and artificial replanting.

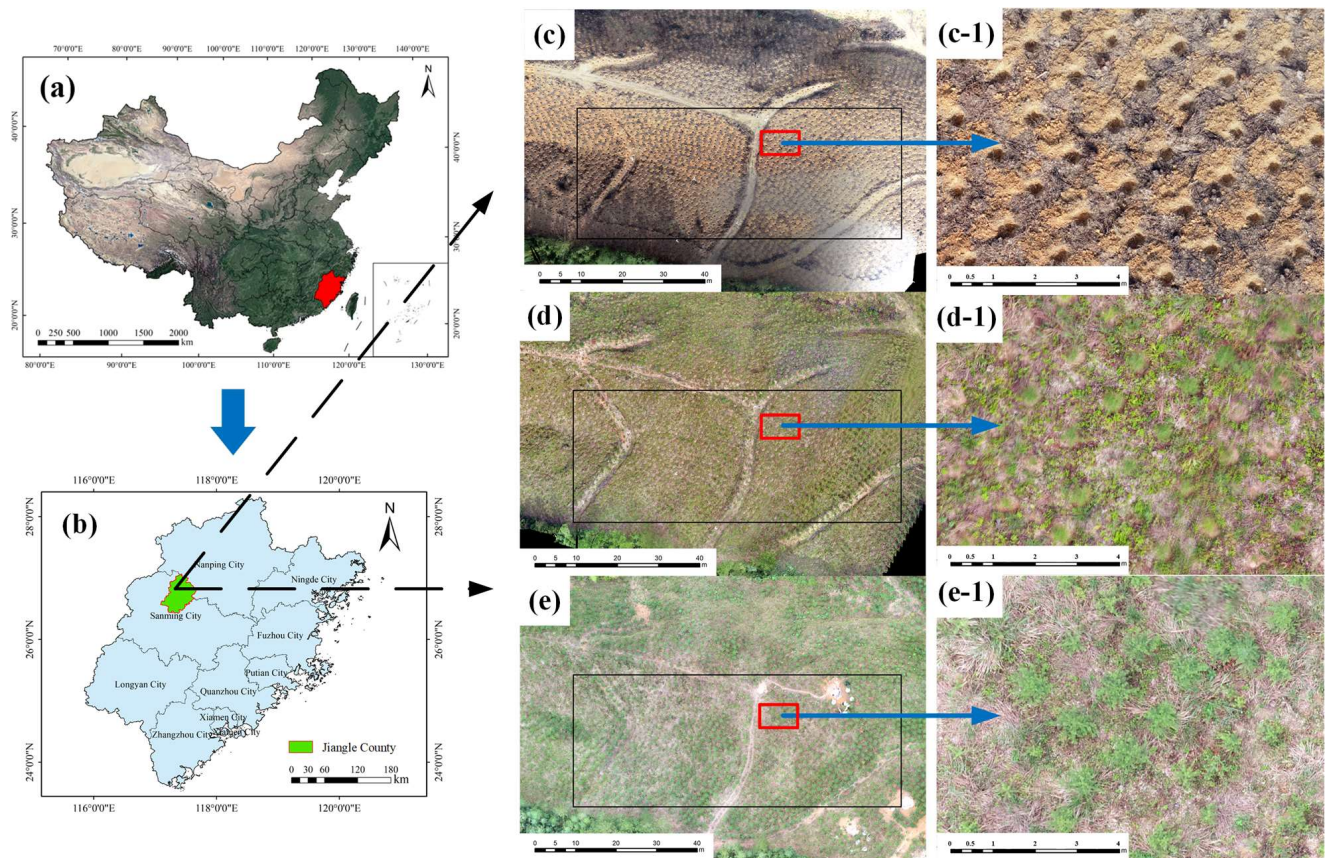


Figure 1. The study region is located in Jiangle County, Fujian Province, China. (a) Map of China; (b) Jiangle County, Fujian Province; (c) UAV image of tree pit on 22 January 2019; (d) UAV image of young forest on 2 October 2020; (e) UAV image of young forest on 2 October 2021; (c-1,e-1,d-1) are magnified images in red rectangle region in (c–d).

2.2. Field Survey

The field measurement data was obtained using a GNSS receiver, a tape measure, a measuring rod, and a laser altimeter. A GNSS receiver was used to collect ground point elevation information in the measurement process, which was a convenient way for verifying the ground elevation accuracy. Tree heights' samples were collected in the field by measuring the difference from the bottom and top of the tree. The tape measures, laser altimeter, and retractable measuring rod were used to measure low young trees samples one and two years after afforestation in 2020 and 2021, respectively. In addition, to ensure representative samples of saplings, we collected 45 tree-height samples in 2020 and 2021 (Figure 2). For each tree, we recorded longitude, latitude, and elevation coordinates derived by the GNSS receiver. The measured tree height data were used to verify the accuracy of the result from UAV RGB images.

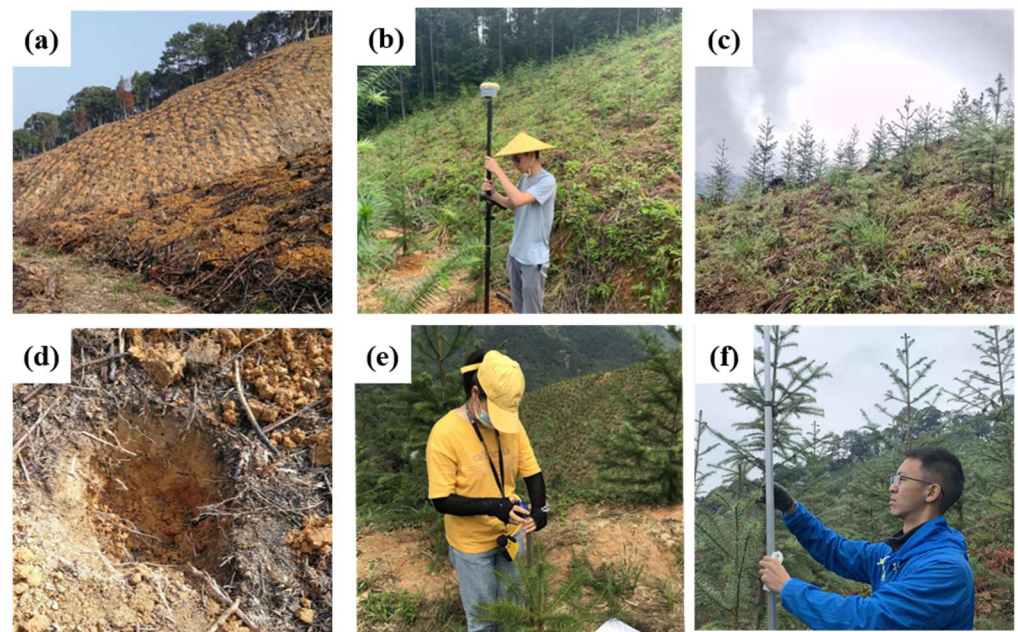


Figure 2. Field measurements of the scene. (a–c) shows the scenes of the test region in 2019, 2020, and 2021, (d) is the tree pit before afforestation in 2019, and (e,f) is the field scenes for tree height measurement in 2020 and 2021.

2.3. UAV Images

The flight was carried out with DJI products (Da-Jiang Innovations, Shenzhen, China) to collect data, including DJI Phantom 4, DJI Mavic 2 and DJI Phantom 4 RTK. Although we used a different types of UAV in light of the update of DJI product over the past few years, the image sensors on all three drones have the same 1-inch 20-megapixel lenses, among which DJI Phantom 4 RTK has flight capabilities parallel to the slope. It flies at a relatively constant altitude according to ground slope.

The UAV was set to hover in the flight path direction keeping the image sensor facing 90° vertically downward until the end of the flight. During the hovering, the UAV's image sensors took pictures continuously throughout the course. The route planning dates were 22 January 2019, 2 October 2020, and 2 October 2021. The flight height was found to be optimal within a range of 30 to 40 m above the forest canopy based on the survey and the flight time. To ensure the accuracy of height estimation of young trees, the overlap rate of the flight paths was no less than 80%. For the tree pit images from 2019, young forest growth images were obtained in 2020 and 2021. Specific flight parameters are provided in Table 1.

Table 1. Flight parameter.

Flight Time	UAV Model	Flight Height	Forward Overlap	Side Overlap	Number of UAV Photos
20190122	DJI Phantom 4	40 m	90%	80%	335
20201002	DJI Mavic 2	30 m	90%	80%	1167
20211003	DJI Phantom 4 RTK	40 m	90%	80%	574

Image preprocessing was performed in the proprietary Pix4D software (Pix4D, Lausanne, Switzerland), including removing blurry photos, marking ground control points, calculating a dense point cloud, generating DSM data, etc. Later, we obtained the DOM, DSM, and UAV image point cloud. Figure 3 is a DEM derived from the UAV images point cloud (a) and 3D visualization of a UAV image in 2021 overlaid with DEM (b) in the study area. From 2019 to 2021, the image resolution was 0.010 m pixel⁻¹, 0.008 m pixel⁻¹, and

0.015 m pixel⁻¹. To ensure data uniformity, all samples were resampled to 0.015 m pixel⁻¹ using the nearest neighbor assignment method in ArcGIS.

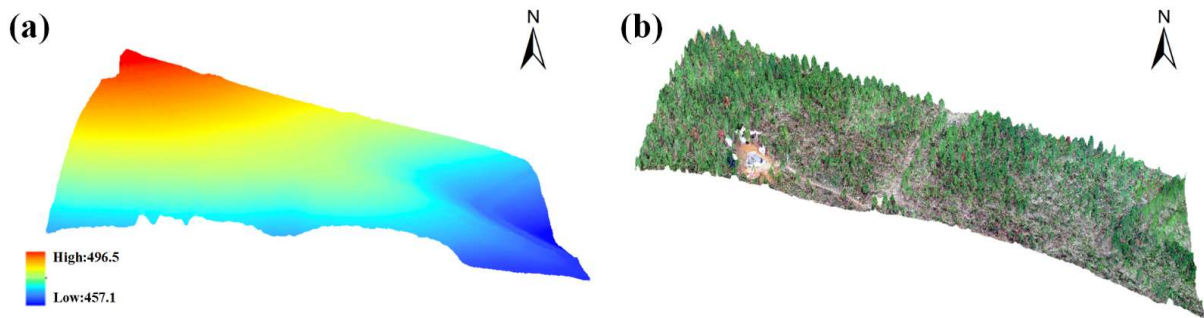


Figure 3. DEM derived from UAV images (a) and 3D visualization of UAV image in 2021 overlaid DEM (b) in the study area.

3. Methods

3.1. Image-Matching Accuracy and Ground Point Accuracy Verification

The center region of UAV image is chosen to reduce the error due to edge deformation of the image. Firstly, we conducted an image-matching accuracy test on the image results obtained in Chap 2.3. We verified the accuracy using random points on the three images. Next, we collected 50 sample points on the DSM using the ARCGIS software and fitted the data linearly. Coefficient of determination (R^2) and root mean squared error (RMSE) were used to describe the fitting effect [Equations (1) and (2)]. The closer R^2 is to 1 and the lower the RMSE, the better the fitting effect. We calculated the root mean square error of the three: the RMSE of 2019 and 2020 images was 0.0546; for 2019 and 2021, it was 0.0493, and for 2020 and 2021, it was 0.0632. The image offset was small and the accuracy meets the test requirements (Figure 4).

$$R^2 = 1 - \frac{\sum_{i=1}^n (y_i - x_i)^2}{\sum_{i=1}^n (y_i - \bar{y}_i)^2} \quad (1)$$

$$RMSE = \sqrt{\frac{1}{n} \sum_{i=1}^n (y_i - x_i)^2} \quad (2)$$

where y_i is the true value; x_i is the predicted value; \bar{y}_i is the mean of the true values; n is the number of samples.

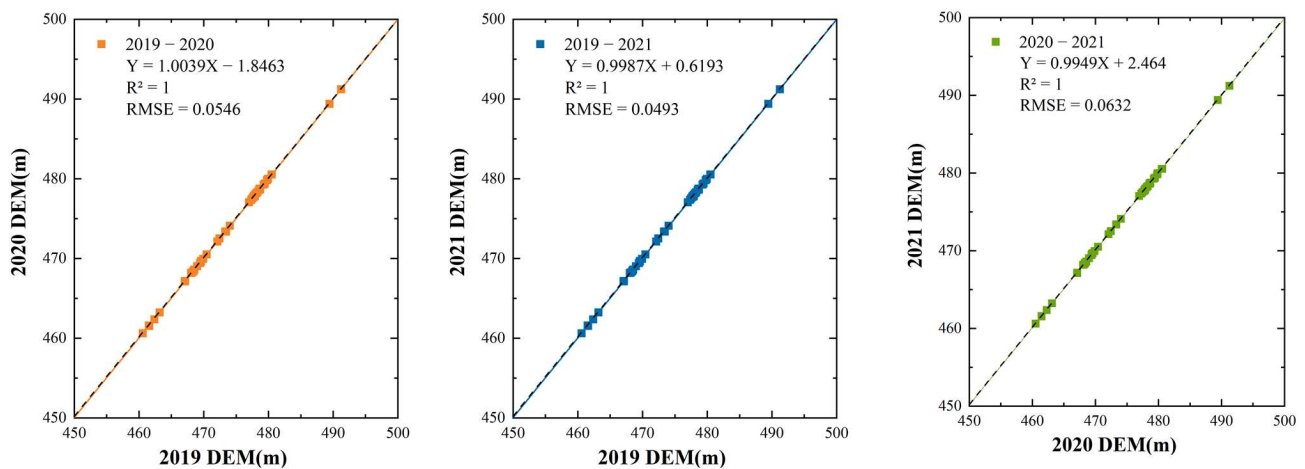


Figure 4. Fitting effect of DEM from different temporal UAV images.

Two kinds of data are used to extract tree height. The first is elevation data based on DSM. This method directly extracts the elevation information of the open ground from the high-precision image. The second is the CHM established by processed DEM. First, we flip the point cloud generated by UAV image mosaic. It then simulates a piece of cloth falling from above onto an inverted surface. The interaction between nodes and point clouds is analyzed and classified into ground points and non-ground points [31]. The DEM processing procedure separates ground and non-ground points from the image-normalized point cloud using a cloth simulation filter (CSF) algorithm. The CSF algorithm performs ground-point classification in the image-normalized point cloud via simple and easily utilized parameters. The parameters are as follows: 1. Cloth resolution (the size of cloth that covers the terrain). 2. Max iterations. 3. Classification threshold (the threshold between ground points and non-ground points). After the image ground point cloud, the DEM elevation data are obtained directly via image interpolation. Since the UAV image from 2019 contains tree pits with 30–40 cm depth, we use the DEM in 2020 as the ground elevation. In this study, all the ground points were used to extract the height of the young forest based on the ground elevation in 2020.

We used 140 ground verification points in the ground elevation accuracy verification data in Figure 5. The RMSE of DEM separated by the cloth simulation filter algorithm and measured DEM is 0.0786. The RMSE of image DSM and measured DEM is 0.0513. In comparison, the ground point elevation in the DSM image of 2020 has higher accuracy than the ground point elevation separated by the cloth filtering algorithm.

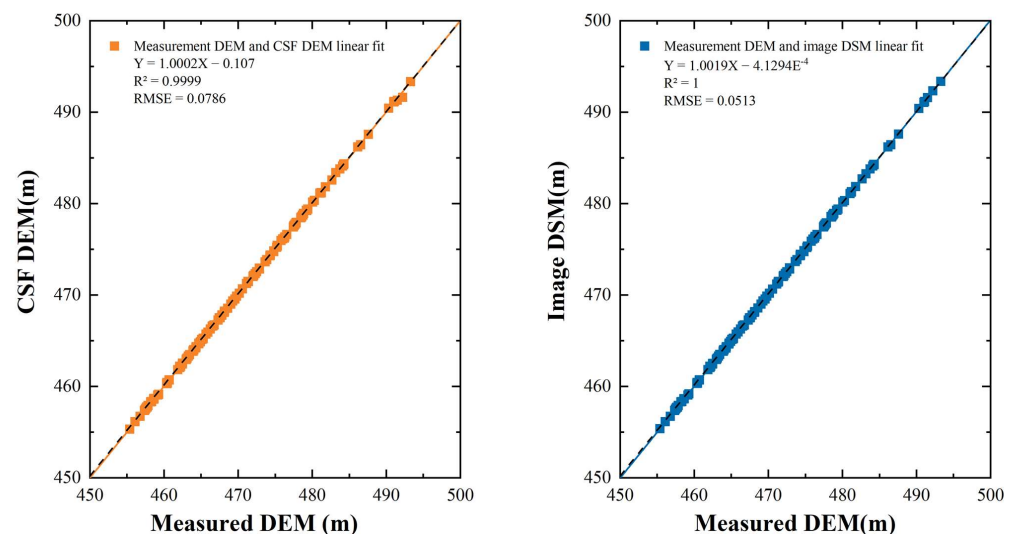


Figure 5. Accuracy verification of ground point for DEM.

3.2. Tree Pits Extraction

In DSM images, the edges of tree pits display drastic changes in image gray value, texture, and other features. The position of tree pits was extracted from DSM images through Canny edge detection and circular Hough transform [32]. As a multi-step algorithm, the Canny edge detection algorithm consisted of four sections [33]. First, Gaussian filtering is used to reduce image noise, smoothing the image and increasing the width of the image edge information. Secondly, the gradient value and gradient direction of the image were calculated to represent the change degree and direction of the gray value. Thirdly, non-axial suppression was performed and the region with the greatest change in gray level was maintained. Its pixel was set to one, and the remaining pixels were set to zero. Finally, double thresholds were set to screen pixel edges, and low and high thresholds were set to retain edge pixels in the field, while others were eliminated.

Hough transformation is a form of feature detection, which is generally used to identify straight lines in images. The circular Hough transformation changes the detected object

from a straight line to a circle. By detecting the edge image after Canny edge detection, the position of the circle in the image was extracted, and then the position of the tree pit was obtained. The basic principle of circle detection is as follows in Equations (3)–(5).

$$(x - a)^2 + (y - b)^2 = r^2 \quad (3)$$

$$x = a + r * \cos(\theta) \quad (4)$$

$$y = b + r * \sin(\theta) \quad (5)$$

where (a,b) is center of the circle; r is the radius; θ is the angle.

The circular pit at the edge of the pit was detected via Canny edge detection, and the circle Hough transform was used to find the circle. The tree pit was vectorized through the Opencv_python-4.0.1.23 language package to determine the approximate position of the tree well. To ensure the accuracy of monitoring of young forests in the test region, the location of tree pits was manually calibrated in all test regions. We manually corrected the missing and incorrectly extracted tree pits to ensure accurate correspondence to each seedling. A total of 1044 saplings were detected in this study.

Tree vertices and ground points had to be included in the tree pit vector region, which needed to be optimized. The buffer size is determined by measuring the sapling canopy size in the DOM image, and there was no area overlap after the tree pits were buffered. After two stages of image testing, the results of 0.25 m and 0.45 m expansion were obtained. After comparison, a circle with a radius of 0.45 m has a relatively complete tree crown and clear ground point information, and there is no overlap. Finally, an expansion of 0.45 m was selected as the location of the tree pit for each tree's position (Figure 6).

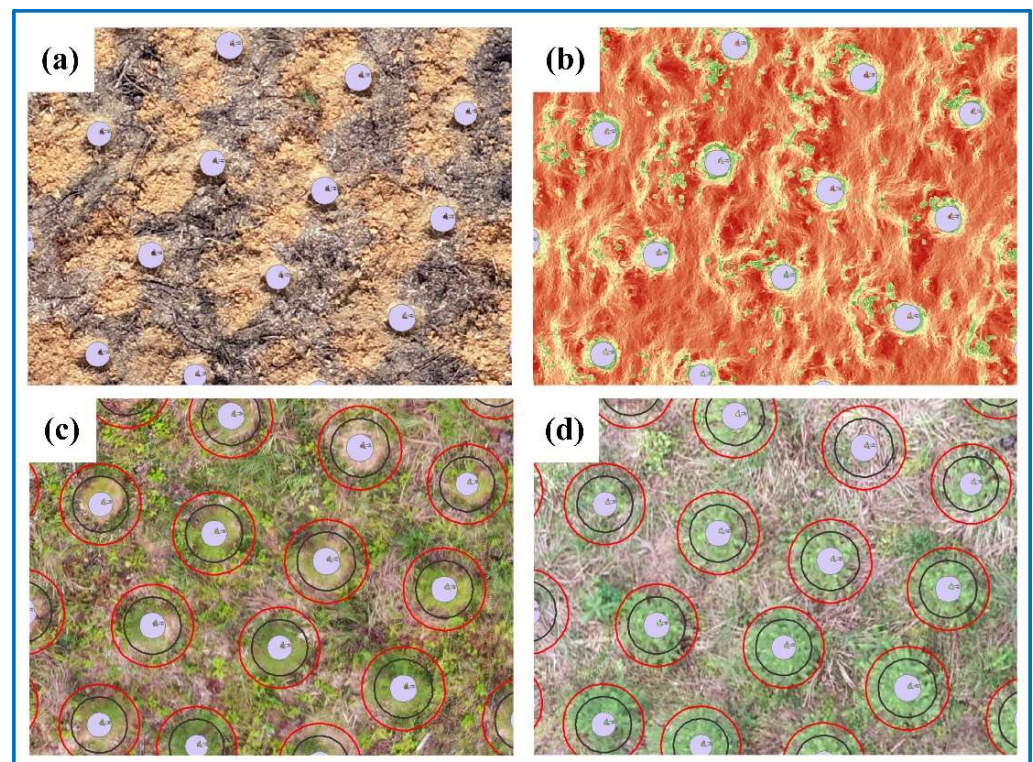


Figure 6. The location of tree pit and the determination of registration. (a) shows automatically obtained tree pits shapefile; (b) shows the result of manual correction; (c) shows optical UAV imaging in October, 2020; (d) shows optical UAV imaging in October 2021. The process of obtaining the location and size of tree pits, the red circle is the result of the 0.25 buffer and the black circle is the result of the 0.45 buffer.

3.3. Tree Height Extraction Based on Divide and Conquer Algorithm

The images are stored in a computer as a digital matrix. The numbers are called pixel values, and the divide and conquer method classifies these numbers into components. Thus, the enhancement and information of image naturalization and detail are obtained [34,35].

Figure 7 shows the tree-height extraction process by the divide and conquer algorithm. UAV images were processed using a divide-and-conquer method for extracting tree height information. First of all, the image was cut in batches according to the vector position through modeling. The model cut the original DSM data in accordance with each tree pit buffer. Secondly the clipping results of each tree pit were numbered according to the File Identifier Descriptor (FID) of the buffer for later correspondence. Finally, the pixel values of the DSM data in each tree pit were sorted and edited into a separate array to search for the maximum and minimum values in the array. When the number of each group is less than or equal to two, the equal division is no longer carried out. The tree top and ground points were determined by searching the maximum and minimum values in the array.

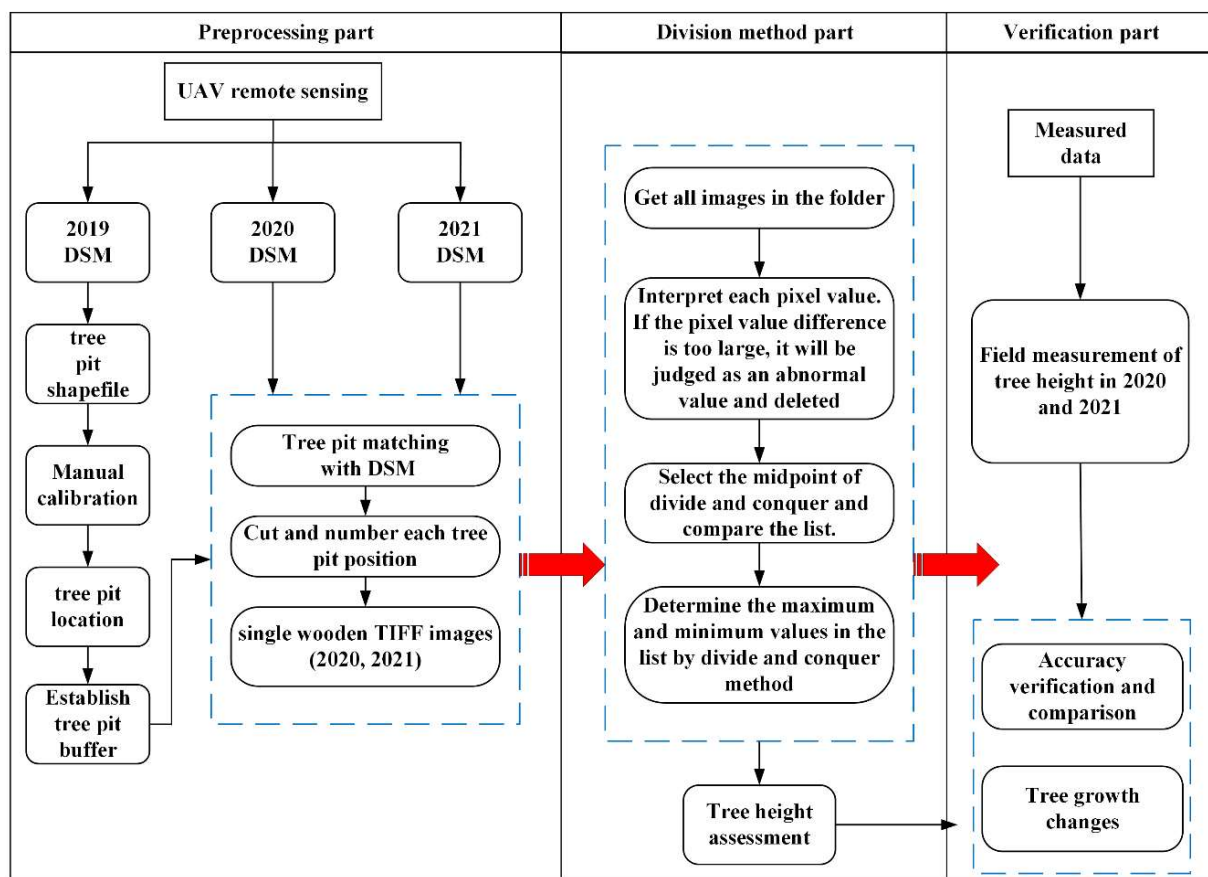


Figure 7. Tree height extraction process via divide-and-conquer algorithm.

The basic idea of divide and conquer is to divide a problem of an N-size problem into smaller K-group problems. By solving the subclass problem, the answer to the initial problem is obtained. The divide-and-conquer method was used to divide the image data in each buffer to obtain the maximum and minimum pixel values. The maximum value is the position of the top bud, the minimum value is the ground point, and the difference between the two is the height of the young tree (Figure 8).

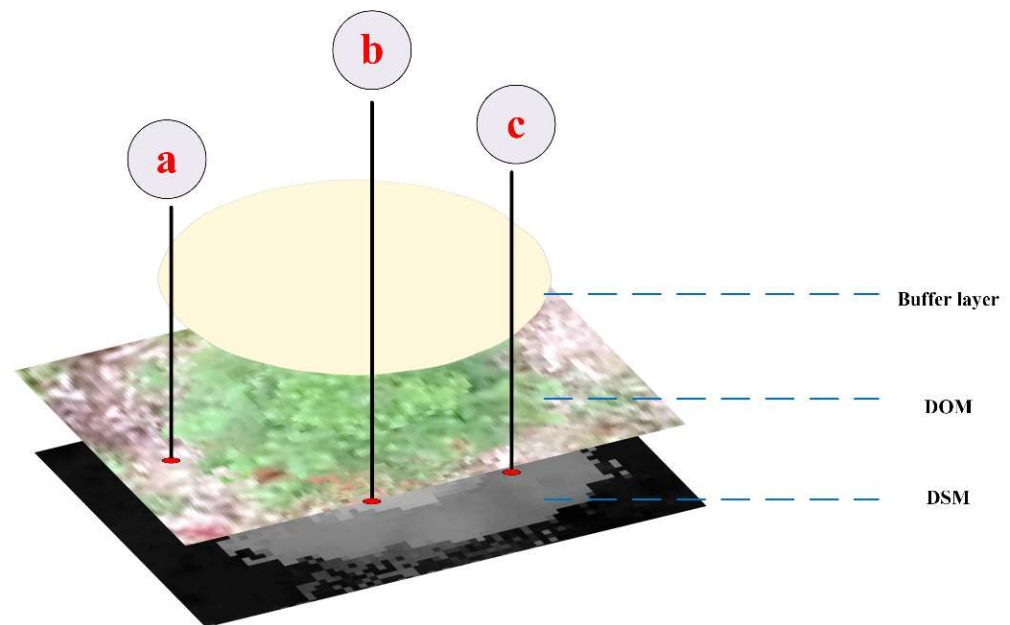


Figure 8. Divide and conquer diagram, where ‘a’ is the regional minimum value (2020): 479.49; ‘b’ is the regional maximum value (2020): 480.10; ‘c’ is the abnormal value (deleted).

In this experiment, we tested the young trees in 2020 and 2021 to determine the yearly growth of young trees. We assumed that the ground elevation information did not change significantly. The estimation of tree height in 2020 and 2021 adopted the ground data in 2020 to ensure the uniformity of DEM data.

3.4. Tree Height Extraction Based on Local Maximum Algorithm

In 2020, most young seedlings were about 1 m in height, and some young seedlings with poor growth were less than 1 m in height, which makes it difficult to build precise CHM. In addition, we found many incorrect references and missing extracts when searching for treetop windows from CHM in 2020 using a local maximum algorithm, according to our experiments. Thus, the local maximum algorithm was used to extract the young trees in 2021, but not in 2020.

The CHM was obtained by subtracting the DEM by DSM. The local maximum algorithm for the established CHM image was identified and located using the IDL software package. In the extraction process, the different window sizes affected the extraction results of sapling tree vertices, which indirectly resulted in the accuracy of tree high estimation. Thus, the optimal window size had to be derived. The size of the window was justified by the ratio of the average crown diameter of young trees and image resolution (Equation (6)). The average crown size was calculated using the north–south and east–west crown directions.

$$M = \frac{(d1 + d2)}{2p} \quad (6)$$

where M is the window size; $d1$ is the diameter of the DOM to the north–south direction of the forest crown; $d2$ is the diameter of the DOM to the east–west direction of the forest crown; p is a single-pixel resolution size.

After determining the window size, the location and top of the single tree were derived based on the local maximum algorithm. The processing steps were as follows: First, the CHM image was smoothed via Gaussian filtering. Second, the maximum pixel value in the window was extracted according to the window size selected by moving. Finally, the position of the treetop was obtained by vectorizing the maximum pixel in the window, which resulted in a value of zero, and the parameter information was obtained by

extracting pixel values from CHM to treetops using the median value extraction to point tool of ArcGIS software.

3.5. Tree Height Extraction Based on Divide and Conquer Algorithm

In order to evaluate the reliability of the remote sensing tree height and tree density, the extracted tree height was compared with the actual tree height, and the monitoring results were evaluated via the determination coefficient (R^2) and root mean square error (RMSE). In addition, the survival rate was used to evaluate the actual growth of saplings in the plot based on the given tree height and tree growth results (Equation (7)).

$$SR = \frac{SN}{TN} \times 100\% \quad (7)$$

where SR is tree survival rate; SN is the number of surviving trees; TN is the total number of trees.

4. Results

4.1. Extraction Results of Tree Heights and Accuracy Evaluation

In this study, the divide-and-conquer method was used to extract the young tree heights in 2020 and 2021, and the local maximum algorithm was used to extract the young tree heights in 2021. We compared the accuracy of the extracted tree height with the measured tree height and calculated the determination coefficient and root mean square error to evaluate the extraction accuracy. The higher the R^2 , the lower the RMSE, and the higher the accuracy of tree-height extraction. In studies that utilized the same method, there is a correlation between the extracted results and the measured results. In the tree-height result from DAC method, the average tree height in the research region was 1.1284 m in 2020, and the average tree height in 2021 was 2.3677 m (excluding death and damage to the young trees).

The results showed that the actual height of the young forest was the critical factor affecting the accuracy of tree-height extraction. The study found that the taller trees had a better extraction result than the shorter trees. In the research, 40 trees were used for verification. The young tree height ranged from 0.37 m to 2.51 m and the extraction height ranged from 0.27 m to 2.43 m in 2020. The young tree height ranged from 1.35 m to 4.3 m and the extraction height ranged from 1.39 m to 4.27 m in 2021. The experimental results show that the tree height extracted in 2020 deviated significantly from the measurement results, with an average error of 0.17 m and accuracy of 51.73% to 98.99%. However, the height accuracy of most trees extracted using this method was above 80%. In 2021, the extraction accuracy was higher, with an average error of 0.13 m and accuracy between 85.29% and 99.92%. This method's tree-height extraction accuracy is above 90%.

Figures 9 and 10 show that the tree-height detection results in 2021 (mean accuracy = 95.07%, $R^2 = 0.9659$, RMSE = 0.1609) were nearly 11% higher than those in 2020 (mean accuracy = 85.65%, $R^2 = 0.8428$, RMSE = 0.2459). When the absolute error is close, the higher the sapling height, the higher the relative accuracy. On the contrary, the lower the true seedling height, the greater the relative error of extraction. This also affects the precision.

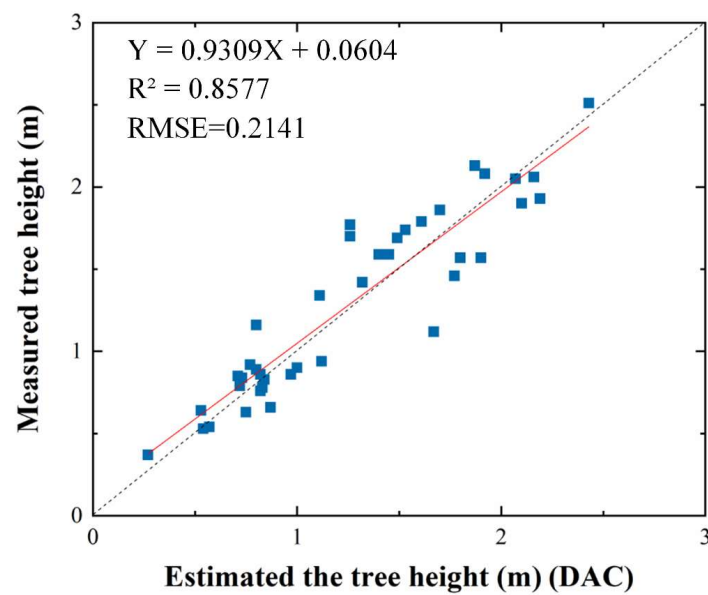


Figure 9. Tree-height accuracy verification; the blue points are the verification results of DAC in 2020.

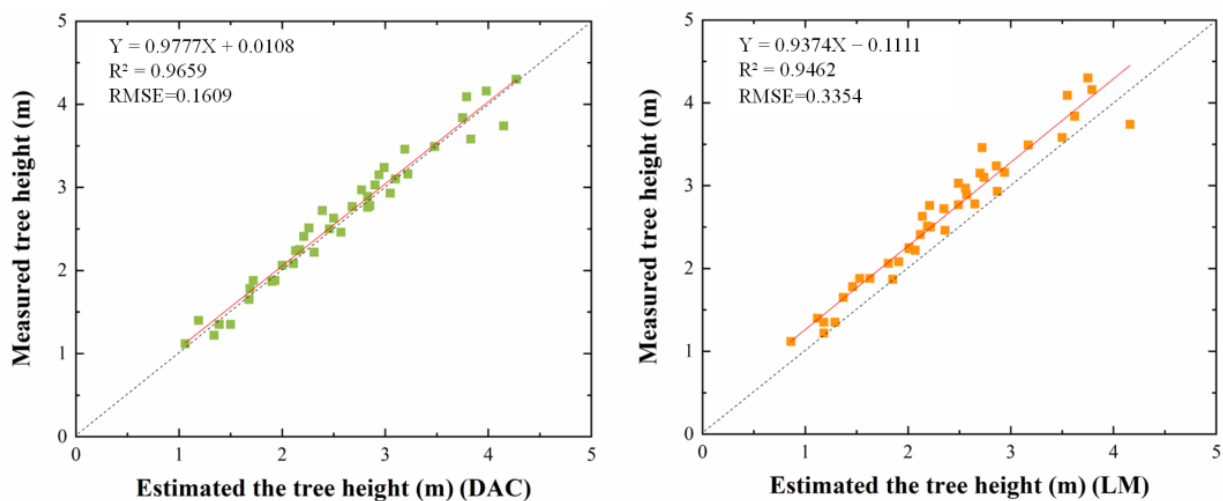


Figure 10. Tree height accuracy verification; the green points are the verification results of DAC in 2021; the orange points are the verification results of LM in 2021.

Secondly, we compared the evaluation performance of this method in young forest. We also used the conventional local maximum algorithm for comparative experiments. Since the local maximum algorithm could not extract the height of the young forest that was too low, we only conducted a comparative test for the extraction results from 2021. During the experiment, we selected 60 pixels as the moving window size parameter to determine the position of a single tree in the research region in 2021. The result of automated treetops' detection was compared with the actual results (Figure 11). The accuracy of the test was 86.8% based on the collection of 1203 tops. There were 159 false points due to weeds covering the road and some young trees showing double tops [36]. To determine the height of young trees with multiple vertices in the experiment, we selected the highest top among the young trees to extract the tree height. As there was no detectable point in the blank region on the road, some false detection points occurred. This did not affect the assessment of single-tree height, and the detection result did not produce false positives. We eliminated the miscommunication point by overlapping the tree pit buffer.

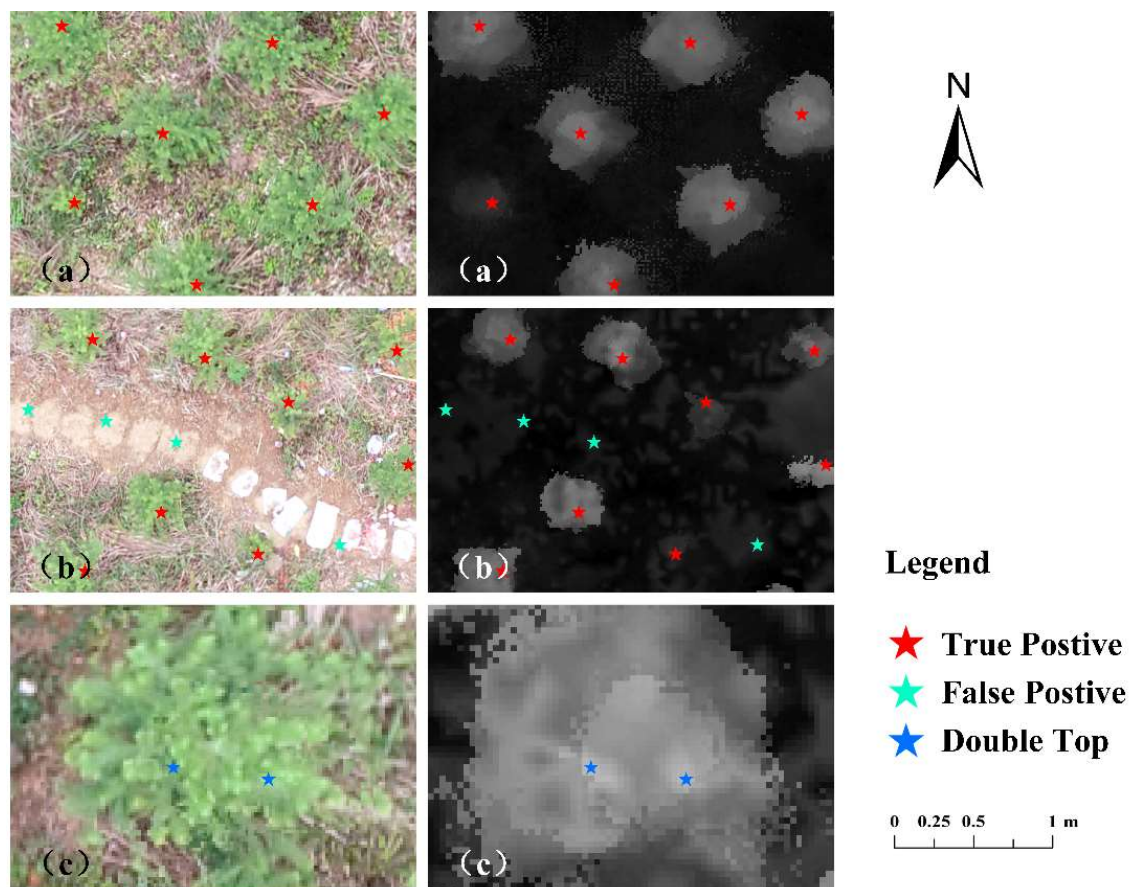


Figure 11. Local maximum value algorithm extract tree crown top; figure (a) shows red stars as true positives; figure (b) shows green stars as false positives; figure (c) shows blue stars as double tops.

Tables 2 and 3 show the accuracy verification of the tree height. The average tree height in the research region was 2.35 m (excluding death and damage to young trees) through the divide-and-conquer and local maximum value methods. The performance of the test results (average accuracy = 88.49%; $R^2 = 0.9462$, RMSE = 0.3354) was marginally inferior to divide and conquer. The R^2 correlation was comparable, whereas the RMSE value was large; the average tree height in the research region was 0.28 m taller.

Table 2. Accuracy verification of tree height in 2020 from DAC.

2020 Tree NO.	Measured Tree Height (m)	DAC (m)	Error	Relative Accuracy (%)
1	1.34	1.11	0.23	82.61
2	1.57	1.90	−0.33	79.09
3	1.70	1.26	0.44	73.99
4	0.78	0.83	−0.05	93.79
...
39	0.64	0.53	0.12	81.67
40	1.42	1.32	0.10	93.23
average	1.29	1.26	0.03	85.89

$R^2 = 0.8577$ RMSE = 0.2141

Note: Error = Measured tree height – Extracted tree height; Relative accuracy = $1 - (|Error| / True\ value \times 100\%)$.

Table 3. Accuracy verification of tree heights in 2021 from DAC and LM.

2021 Tree NO.	Measured Tree Height (m)	DAC (m)	LM (m)	Error of DAC	Error of LM	Relative Accuracy of DAC (%)	Relative Accuracy of LM (%)
1	3.15	2.94	2.70	0.21	0.45	93.19	85.76
2	2.97	2.77	2.56	0.20	0.41	93.43	86.16
3	1.35	1.39	1.18	−0.04	0.17	96.93	87.16
4	3.46	3.19	2.72	0.27	0.74	92.10	78.67
...
39	3.49	3.48	3.17	0.01	0.32	99.70	90.88
40	4.16	3.98	3.79	0.18	0.37	95.67	91.18
average	2.63	2.58	2.35	0.05	0.28	94.87	88.49
				Divide and conquer: $R^2 = 0.9659$	RMSE = 0.1609		
				Local maximum: $R^2 = 0.9462$	RMSE = 0.3354		

Note: Error = Measured tree height – Extracted tree height. Relative accuracy = $1 - (|Error| / True\ value \times 100\%)$.

4.2. Annual Growth Change of Saplings

As seedlings reach a particular height, their growth accelerates dramatically. After afforestation, the invasion of environmental weeds and human damage, as well as the interference of other variables, causes the death of saplings. Afforestation survival rate and preservation rate of afforestation seedlings are two important indicators of afforestation effect. The survival rate refers to the ratio of the number of surviving saplings after one year of afforestation to the total number of saplings planted. The afforestation preservation rate refers to the ratio of the number of retained saplings to the total number of saplings planted after 2–3 years of afforestation. Moreover, the survival rate is close to the preservation rate if trees develop well, and forest management and operation are effective.

The growth status of the young forest can be determined according to the change in tree height (Figure 12). In this study, changes in tree height were determined using the DAC algorithm. Saplings were transplanted in the study area between March and June 2019, and the average above-ground height of saplings was measured at about 10 cm in the field. The height changes of sapling growth could be obtained through two temporal high-precision UAV remote sensing images taken on 2 October 2020 and 2 October 2021. In order to evaluate the health status of young tree growth, in the first year of growth, an increase in height of less than 0.2 m was regarded as tree death, and the trees were then divided into groups of equal height. The difference between the extraction results of tree height in the second year and the initial height was the annual growth height change.

The results demonstrated that there were 59.20% trees growing below 1.0 m and 45.88% trees growing above 1.0 m in Figure 13. In addition, we estimated the death and growth of young trees between 2020 and 2021 by comparing the height of young trees. Only one tree died in 2020. The average growth height of trees was 1.03 m, with a maximum growth height of 2.85 m and a minimum growth height of 0.21 m. Among them, the survival rate of young trees in the second year was 99.99%, which is consistent with the field survey data of 95%. In 2021, there were 32.76% trees growing below 1.0 m and 52.76% trees growing above 1.0 m. Some manual damage and natural deaths occurred due to artificial interference; thus, dead and damaged trees account for 14.37% of the total number of trees in the test area. The average growth height of trees was 1.19 m, with a maximum growth height of 3.10 m and a minimum growth height of 0.21 m. The preservation rate of the test region was just 85.63% due to the impact of manual damage and natural conditions during the third year.

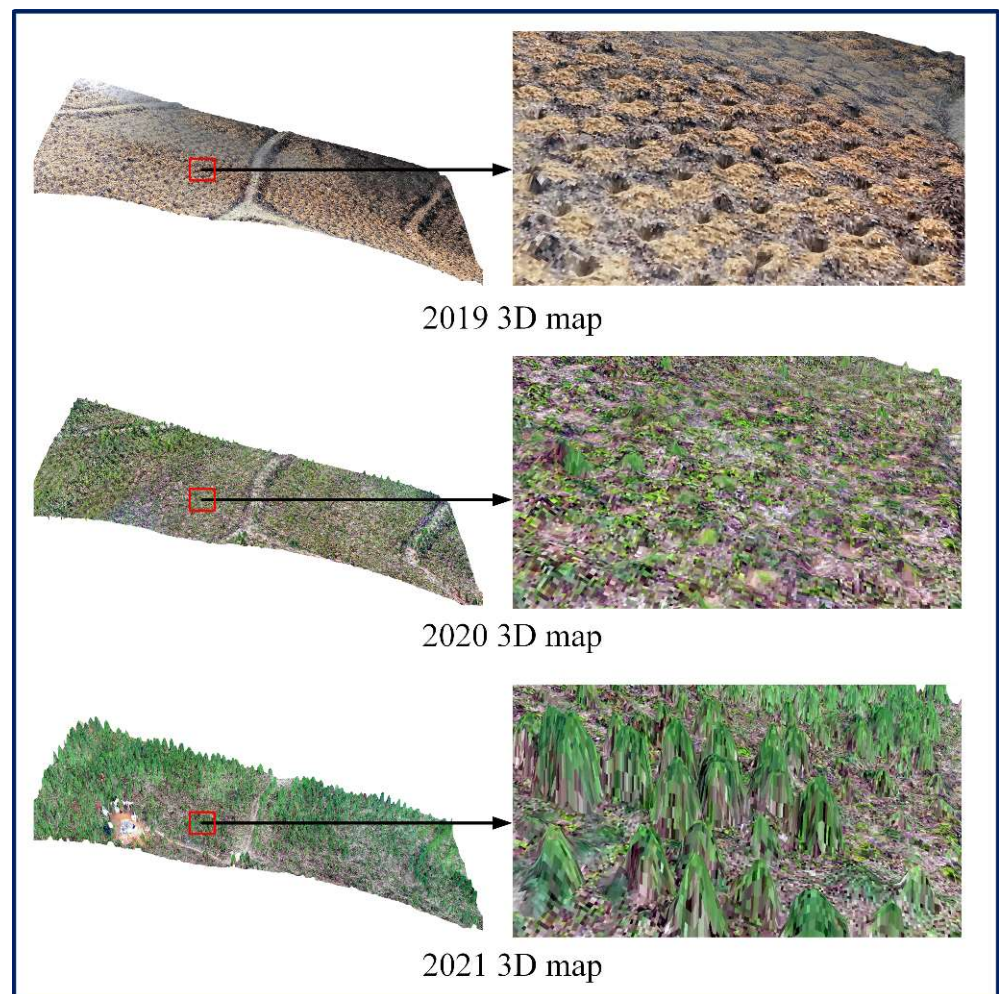


Figure 12. Young forest height changing 3D map based on UAV image point cloud.

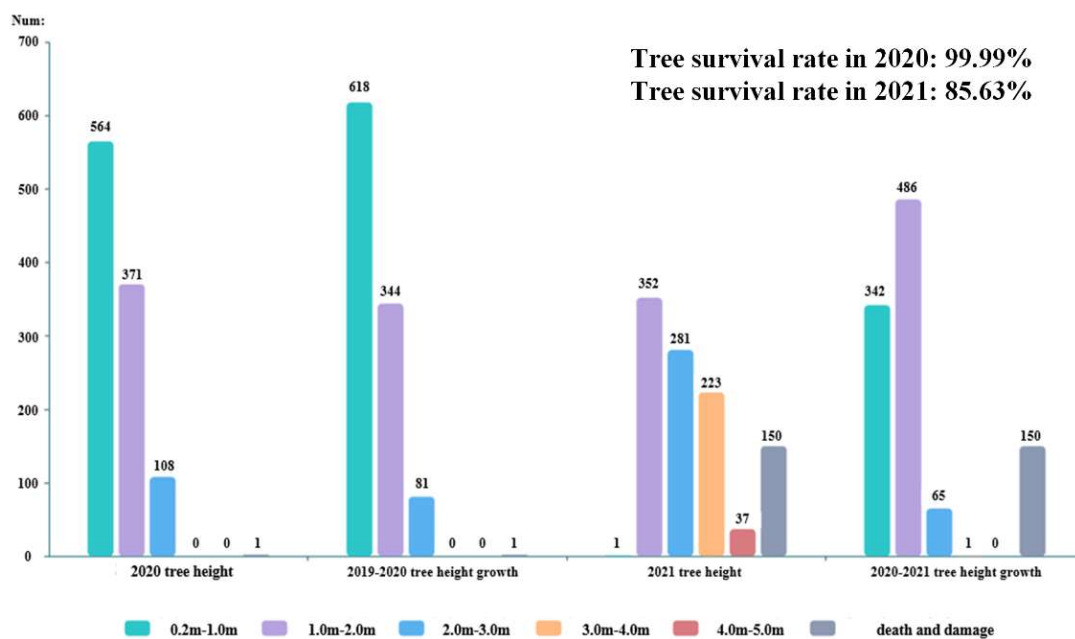


Figure 13. The different heights and growth of the young trees from 2019 to 2021.

Figure 14 shows the average monthly growth boxplots and the cycle growth boxplots for 2020 and 2021. The growth time from 2019 to 2020 is 4 months longer than that from 2020 to 2021. The total number of surviving trees is n value, 2020: $n = 1043$; 2021: $n = 894$. In addition, the boxplot expresses the maximum and minimum tree heights, upper, lower quartiles, median, and outliers that grow too quickly. The median monthly average growth rate in 2020 was 5.25 cm, and the median monthly average growth rate in 2021 was 10.35 cm. The median monthly growth in 2021 was nearly double that in 2020. In addition, the monthly growth of the surviving single trees in the region after afforestation was calculated. After afforestation, the median monthly average growth rate of the region was 7.22 cm, which was in the middle of the growth in 2019 and 2020.

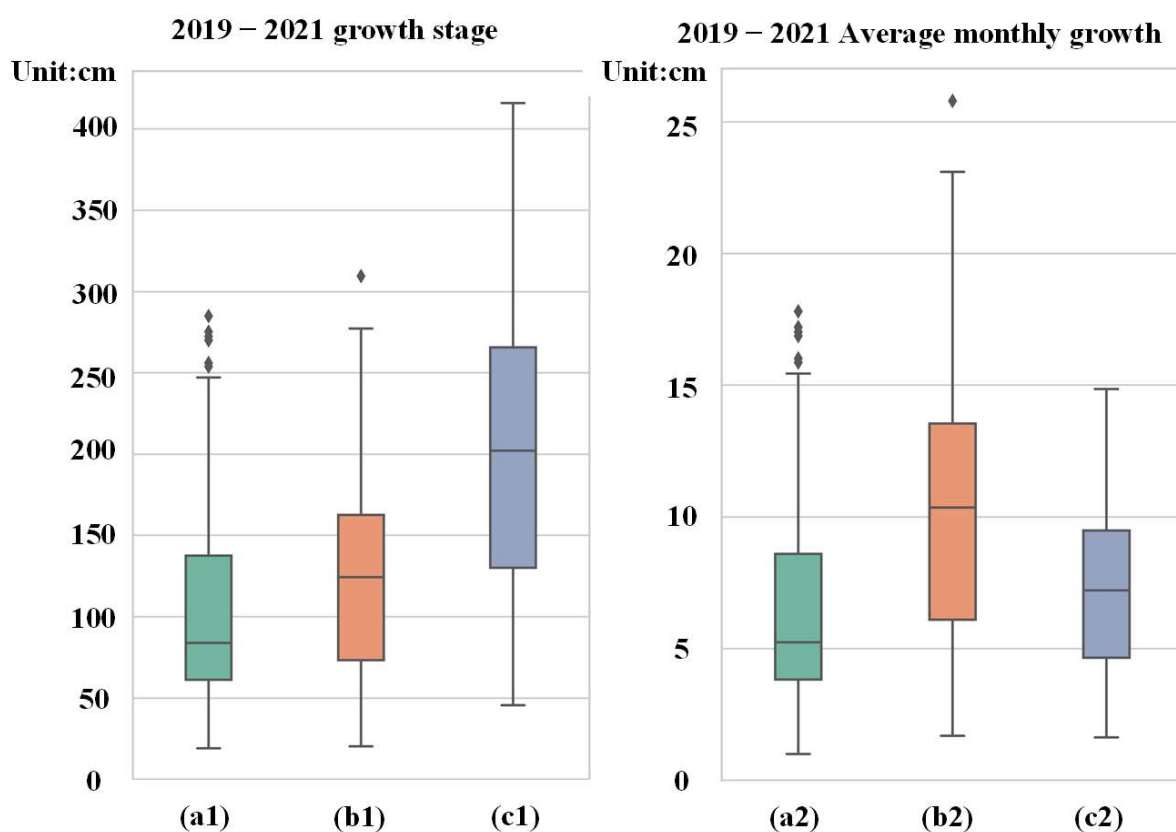


Figure 14. The left boxplot shows the annual growth of the saplings from 2019 to 2021, and the right boxplot shows the average monthly growth of the saplings each year. The colors of the boxplot show the different stages of young tree growth. Green shows the survival of young trees from June 2019 to October 2020 ($n = 1043$); orange shows the survival of young trees from October 2020 to October 2021 ($n = 894$); gray shows the survival of young trees from June 2019 to October 2021 ($n = 894$). The median of the (a1) boxplot was 83.95 cm; the median of the (b1) boxplot was 124.25 cm; the median of the (c1) boxplot was 202.03 cm; the median of the (a2) boxplot was 5.25 cm; the median of the (b2) boxplot was 10.35 cm; the median of the (c2) boxplot was 7.22 cm.

In particular, except for a few saplings that grew rapidly in 2019–2020, most saplings grew at a slower rate than the previous year, indicating that young trees inhibit top growth and promote root growth when they start growing. Additionally, when young trees reach a certain height, root growth is inhibited and top growth is encouraged [37]. The health of young forests can be quickly assessed based on growth parameters at the single-tree level (Figure 15). Furthermore, the majority of tree species experience rapid growth rates early in the year (spring) and slow or static development in the summer, autumn, and winter [38]. This study calculated the growth time as of June 2020, missing the rapid growth stage, which could impact the growth rate of young trees from June 2019 to October 2020.

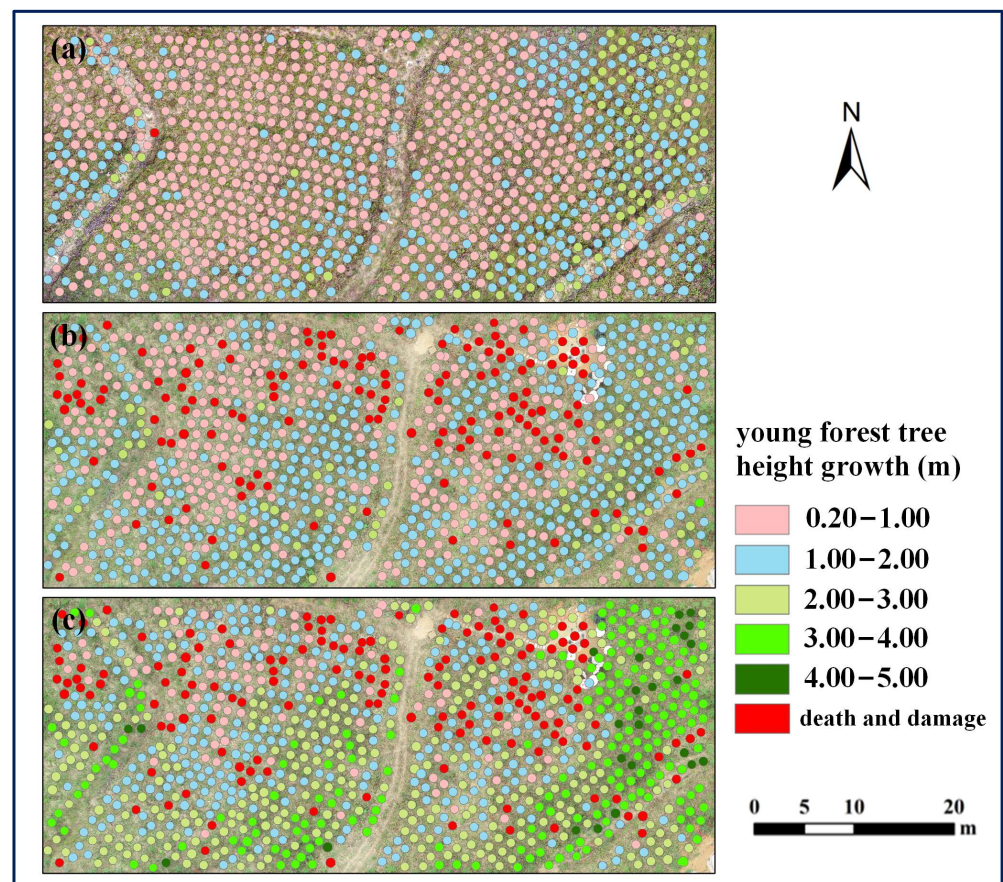


Figure 15. Dynamic change of tree growth. (a–c) show changes in young forest height growth at single tree level at different stages from June 2019 to October 2020, October 2020 to October 2021, and June 2019 to October 2021. The color indicates an additional amount of growth. The pink growth range is 0.2–1.0 m; the blue growth range is 1.0–2.0 m; the light green growth range of 2.0–3.0 m; the green growth range is 3.0–4.0 m; the dark green grows in the 4.0–5.0 m range. According to (c), the growth of 0.2–1.0 m in three years is poor; 1.0–2.0 m growth medium; 2.0–4.0 m is healthy growth; above 4.0 m is considered very healthy.

The measurement values were randomly selected according to the visibility of treetops in the study area. The correctness of the data is ensured by directly comparing the extracted and measured tree heights. Considering the reliability of the research results, the extracted results were compared with the existing results. In the case of the same species, several researchers have identified the period of high development between May and August. The average growth rate of fir is 68 cm [38]. In less than two years, the growth height of the young fir is between 1.13 m and 3.05 m [15]. In this study, the young trees were 0–2.5 years old, and the lowest growth was 0.71 m. The maximum growth is 4.90 m and the average growth is 2.15 m, which is basically the same as the normal growth level of a young fir.

5. Discussion

This work demonstrates the feasibility of using UAV images to capture height changes of young artificial forests. The efficiency of the UAV platform is expected to meet the growing demand for high-precision imaging and data-collection efficiency. There are two kinds of UAV platforms: LiDAR and consumer-level UAV RGB images. Compared to consumer-level UAVs RGB images, UAV LiDAR is expensive and inconvenient. Lidar sensors are not particularly compact and have a heavier processing load than optical sensors. In addition, UAVs with LiDAR sensors are greatly larger than those with optical sensors for flight stability. Using consumer-level RGB reduces costs, and it is easy to use in

forestry, but there are enormous challenges in data quality and algorithms. For example, ground elevation information cannot be obtained in forests with high canopy density. Secondly, the low height of young forests makes it difficult to detect treetops, which further increases the difficulty of extracting individual tree height and tree-height variation. This study demonstrates that tree height and a change in single tree level can be efficiently detected via a high-precision RGB image in the growth stage from seedling to sapling.

5.1. Several Aspects in Data Processing

This study used the DJI series of high-resolution UAVs to collect remote sensing data of the same plot for three years. High-resolution DOM can extract tree crowns and classify tree species [39,40], and modeling may be used to extract tree height and determine information such as the forest DBH using high-resolution DSM [41,42]. In this study, we acquired approximately 1.5 cm-resolution DOM, DSM, and image point cloud after the image mosaic. Using the automatic detection algorithm and high-precision image data, tree height extraction and tree height change monitoring were carried out in the open, sparse, and young forest test plot.

In UAV route planning, the overlapping rate of UAV flight and the altitude of the flight may impact the image as well as image mosaic quality. For instance, the higher the overlap rate and the lower the flying height, the more precise the resulting mosaic image. Extensive collection parameters can supply more cloud points, which generate images. These cloud points can yield structural forest land parameters. However, the research shows that when the overlap rate and flight height reach a certain threshold, there is little difference between increasing the overlap rate and lowering the flight height and the original collection parameters [43]. Proper overlap and flight height can reduce flight time and the need for UAV batteries. For example, efficiency can be improved by reducing overlap and flight height in cases where tree tops feature prominently.

In terms of UAV data-processing efficiency, although UAV data are measured more quickly than on-site data, the time cost required for data processing and tree height detection increases [44] in Pix4D. It takes about 2–4 h to generate results in Pix4D software, and the processing time depends on computer performance. Secondly, the efficiency of tree height extraction is determined by data quality and algorithm performance. On one hand, modeling, manual calibration, and the DAC approach takes 50 min, while the divide and conquer algorithm only takes 10 s using this process. On the other hand, by separating ground points from non-ground points using a cloth filtering algorithm, the CHM was established, and the local maximum value was extracted from IDL, which significantly increased the research time (4 h). Due to the high resolution of the image, the processing is slow in IDL (2 h). However, both methods can ultimately obtain the tree height.

5.2. Uncertainty about Height Estimation for Young Single Trees

This study shows that UAV data have high feasibility for extracting young forest height. The estimation accuracy of seedling height in the first year was lower than that of the second and subsequent years. The surface of the test area reflected by the DSM image is relatively complex, and the local terrain experiences great fluctuation. In this study, the tree height resulting from the difference in the height of the tree top and bottom was calculated from high-precision UAV DSM images and precise tree pit positions. The principle of the extraction method is similar to that of manual measurement.

The height of seedlings was extracted via the same method in different age and growth states. The DAC method shows better correlation in the height estimation of young forests (R^2 is 0.8428 in 2020; R^2 is 0.9659 in 2021). For comparison, RMSE parameters in 2020 were 1.5 times higher than RMSE indicators in 2021 (RMSE is 0.2459 in 2020; RMSE is 0.1609 in 2021). Better results can be obtained with young trees of greater height (2020 forest level average tree height: 1.1284 m; 2021 forest level average tree height: 2.3677 m). At the tree level (stand-level 2 m–5 m), the extraction accuracy of single-tree young forest significantly improved compared with other studies [28,45]. When UAV extracts 0.2–2.0 m

young forests, there is a drop in accuracy and a loss of precision that can be mitigated by reducing altitude and increasing overlap [43]. These results illustrate the importance of sapling height in tree-height extraction accuracy.

Tree height is easy to underestimate during the evaluation of young forest height. The underestimation of tree height achieved may result from the loss of spatial image resolution at the tree top [46]. Especially for the young forest in 2020, there are 59.2% young trees below 1 m, which makes the extraction of tree height extremely challenging. Low young trees also have low fault tolerance, but tall trees are allowed a wide margin of error. In addition, some studies have demonstrated that a high slope and changes in the four seasons significantly affect the extraction of the height of the tree.

5.3. Different Methods of Young Forest Height Observation

The height extraction of the young forest is determined by both image and algorithm performance. Some scholars use the direct extraction method to obtain the tree height from images and estimate the actual tree height from image DSM [44,46,47]. In addition, as the most prevalent method for extracting tree height, the local maximum method has been cited in numerous studies and performed well in mature forests [17,18,48]. Our tests used two distinct approaches. The first method extracts tree height using the DAC algorithm based on high-precision UAV images and the location of tree pits. The evaluation of tree height mainly focuses on the accuracy of the initial image, which is the basis for extracting the exact tree vertex and root base. The second method uses the local maximum algorithm to extract treetops in CHM. In this process, image point cloud cloth filtering is used to segment ground points and non-ground points, interpolate 3D point cloud data, and calculate the difference between DSM and DEM. In this study, we tested data from 2021. In comparison, the accuracy of direct extraction was significantly improved using the divide-and-conquer method ($R^2 = 0.9659$, $RMSE = 0.1609$). The tree height obtained by the local maximum algorithm performs well in the correlation degree between extraction and measurement but displays a significant error in RMSE accuracy ($RMSE = 0.3354$) compared with the first method.

The first method uses tree pits to locate individual trees. The circular buffer is used to obtain the maximum and minimum values in this position. The advantage of this is that, at centimeter-level resolution, it reduces the absence of treetops and the data loss for interpolation and CHM. The local-maximum value for the lower-height young trees has partial error extraction when performing single tree recognition. There were a great number of extraction results for highly similar regions. For example, many false points appeared in regions with no trees, such as weeds and gravel roads. There may be issues in areas such as Chinese fir, where there are multiple treetops. The local maximum algorithm will extract multiple vertices, creating errors in our individual tree estimation. Second, the CHM is related to the correctness of the local maximum value algorithm. Because of the low height of young forest, it is difficult to obtain high-precision ground elevation information, resulting in the low value of the CHM. Thus, the accuracy of tree height extraction decreases. Studies have demonstrated that the loss of canopy structure can be reduced by improving image resolution [49].

In this investigation, the image resolution is 1 cm, and there is a strong correlation between the field tree height and the measured tree height. The RMSE of a single tree height was good ($RMSE = 0.3354$) and the average accuracy of the single sapling was 88.72%. The DAC method was applied to open, sparse young forests. The original DSM images are decisive to the extracted tree parameters without complex processing. However, the local maximum algorithm is based on CHM, which requires complex filtering, interpolation, and other operations. Each process step may cause small errors, affecting the final tree height precision. Although the performance of the local maximum algorithm is not as good as the DAC method in this area, it can obtain tree parameters more effectively in the area with a lack of single-tree location and high canopy density, while the DAC method can achieve more accurate tree height parameter information in an open and sparse young forest.

5.4. Young Tree Height Variation at Single-Tree Level

Most existing research assessed the growth height and growth status of vegetation based on the forest plot level growth height, and little research has been conducted on the growth of individual trees [30,50,51]. Sapling height growth needs to be measured and calculated independently. However, measuring height changes of individual trees in the field is inconvenient. When trees grow to a certain degree, it is difficult for observers to take field measurements or view the treetops, and high canopy density limits the accuracy and use of environmental monitoring [52]. In addition, since UAV remote sensing can detect the branches and branches of the top crown, it is more convenient to extract tree height based on UAV remote sensing rather than manual measurement in the field.

The production of dynamic changes in the forest drove the composition of biomass and species [53]. As a result of changes in climate and land use, forest parameter levels are also shifting. After afforestation, we evaluated the significant changes in tree populations. The results of this study demonstrated that UAVs can automatically estimate the growth of single trees through high-resolution images. The results demonstrated different growth rates of tree height from June 2019 to October 2020, and from October 2020 to October 2021.

In general, the growth rate of seedlings in the second year was higher than that in the first year, which was consistent with the normal growth characteristics of young woodland. Furthermore, existing literature shows that most external driving factors and interference will affect the growth of trees [54,55]. For example, after cutting and weeding in the young forest region, the utilization rate of light was improved. As the frequency of weeding increases, the growth rate of saplings increases significantly [56]. In our study, weeding was more frequent in the middle and later stages. It is possible that this will encourage young trees to develop more quickly (Figure 15).

5.5. Limitation and Future Perspectives

The DAC method improved the accuracy of seedling height determination via UAV RGB remote sensing compared with the LM method. The DAC method improved more than the LM method when the sapling height was lower than about 1.5 m. Secondly, the UAV image can easily obtain the information on ground with low forest density and fewer weeds. This facilitates the implementation of the DAC method. However, when there is a large number of weeds or high canopy density on the ground, UAV data using highly penetrating LIDAR may be required. This is a drawback of this method. When considering the applicability of close-range remote sensing technology, several issues must be considered. In this experiment, the flying altitude of the UAV was reduced in order to improve the image accuracy. First of all, there are certain risks in flight when reducing the altitude in complex terrain area. Secondly, the area covered by single drone flight will be reduced and efficiency of data collection will be affected when the flying altitude of the UAV declines. In future research, different flight heights can be considered to detect the tree height level.

In this study, we evaluated and confirmed the effectiveness of UAV-visible images for estimating height and growth of young trees. However, due to labor cost constraints, we have not collected manual measurements in single wood-level seedlings to validate our results, nor did we discuss the influence of crown amplitude size on height extraction. We hope to collect more field measurements in the future to carry out in-depth research in these areas.

6. Conclusions

This research demonstrates that low-cost consumer UAVs can extract the heights of young forests after afforestation, precisely fulfilling forest survey objectives, and the obtained data can be used to examine the height change of young forests. In addition, the height of smaller saplings can be extracted effectively via assisted high-precision images of tree pits and saplings. Using the local maximum algorithm, the tree height in 2021 was obtained without the use of tree pits, but the tree height in 2020 with a lower height level

could not be obtained. For open, sparse saplings, it may be more efficient and practical to directly record ground points and treetops by taking high-resolution photos. On the other hand, we studied the height changes of individual trees using high-precision images. The health level of young stands and the factors affecting the growth of young stands were evaluated by height growth changes at each stage (tree survival rate in 2020: 99.99%; tree survival rate in 2021: 85.63%).

The study shows that low-cost visible light UAV RGB images can accurately obtain sapling height and individual tree height growth after afforestation through high-precision influence, which solves the problem of high cost and low efficiency of manual investigation. This is a key step towards automated forest management. In this paper, we investigated the effectiveness of detecting height and annual growth of young trees based on UAV RGB remote sensing. Future research needs to be conducted in different regions and with an expanded scope to meet the needs of the large-scale evaluation of afforestation achievement.

Author Contributions: Conceptualization, X.Z.; methodology and software, H.W. and C.C.; data curation, writing—original draft preparation, and visualization, X.Z., H.W. and H.H.; writing—review and editing, H.W. and X.Z.; revising, T.J. and G.N. All authors have read and agreed to the published version of the manuscript.

Funding: This research was supported in part by International Cooperation Project of Fujian Province, China (No. 2022I0007); Industry-university cooperation project of Science and Technology Department of Fujian Province, China (No. 2022N5008).

Data Availability Statement: The data presented in this study are available on request from the corresponding author.

Acknowledgments: The authors would like to thank the Jinsen Forestry Co., Ltd., Fujian, for providing field survey support. The authors also appreciate the valuable comments of the reviewers.

Conflicts of Interest: The authors declare no conflict of interest.

References

1. Ko, C.; Lee, S.; Yim, J.; Kim, D.; Kang, J. Comparison of Forest Inventory Methods at Plot-Level between a Backpack Personal Laser Scanning (BPLS) and Conventional Equipment in Jeju Island, South Korea. *Forests* **2021**, *12*, 308. [[CrossRef](#)]
2. Fan, G.; Feng, W.; Chen, F.; Chen, D.; Dong, Y.; Wang, Z. Measurement of volume and accuracy analysis of standing trees using Forest Survey Intelligent Dendrometer. *Comput. Electron. Agric.* **2020**, *169*, 105211. [[CrossRef](#)]
3. Lan, H.W.; Robert, A.C.; Mark, V.F. An Evaluation of Forest Health Insect and Disease Survey Data and Satellite-Based Remote Sensing Forest Change Detection Methods: Case Studies in the United States. *Remote Sens.* **2018**, *10*, 1184.
4. Maqbool, A.; Mirza, A.; Afzal, F.; Shah, T.; Khan, W.Z.; Zikria, Y.B.; Kim, S.W. System-Level Performance Analysis of Cooperative Multiple Unmanned Aerial Vehicles for Wildfire Surveillance Using Agent-Based Modeling. *Sustainability* **2022**, *14*, 5927. [[CrossRef](#)]
5. Wagner, F.H.; Ferreira, M.P.; Sanchez, A.; Hirye, M.C.; Zortea, M.; Gloor, E.; Phillips, O.L.; de Souza Filho, C.R.; Shimabukuro, Y.E.; Aragão, L.E.O.C. Individual tree crown delineation in a highly diverse tropical forest using very high resolution satellite images. *ISPRS J. Photogramm.* **2018**, *145*, 362–377.
6. Mu, Y.; Fujii, Y.; Takata, D.; Zheng, B.; Noshita, K.; Honda, K.; Ninomiya, S.; Guo, W. Characterization of peach tree crown by using high-resolution images from an unmanned aerial vehicle. *Hortic. Res.* **2018**, *5*, 74. [[CrossRef](#)]
7. Liu, G.; Wang, J.; Dong, P.; Chen, Y.; Liu, Z. Estimating Individual Tree Height and Diameter at Breast Height (DBH) from Terrestrial Laser Scanning (TLS) Data at Plot Level. *Forests* **2018**, *9*, 398. [[CrossRef](#)]
8. Franceschi, S.; Antonello, A.; Floreancig, V.; Gianelle, D.; Comiti, F.; Tonon, G. Identifying treetops from aerial laser scanning data with particle swarming optimization. *Eur. J. Remote Sens.* **2018**, *51*, 945–964. [[CrossRef](#)]
9. Mao, P.; Qin, L.; Hao, M.; Zhao, W.; Luo, J.; Qiu, X.; Xu, L.; Xiong, Y.; Ran, Y.; Yan, C.; et al. An improved approach to estimate above-ground volume and biomass of desert shrub communities based on UAV RGB images. *Ecol. Indic.* **2021**, *125*, 107494. [[CrossRef](#)]
10. Chen, Q.; Gao, T.; Zhu, J.; Wu, F.; Li, X.; Lu, D.; Yu, F. Individual Tree Segmentation and Tree Height Estimation Using Leaf-Off and Leaf-On UAV-LiDAR Data in Dense Deciduous Forests. *Remote Sens.* **2022**, *14*, 2787. [[CrossRef](#)]
11. Asier, R.L.; Lluis, B. Greenness Indices from a Low-Cost UAV Imagery as Tools for Monitoring Post-Fire Forest Recovery. *Drones* **2019**, *3*, 6.
12. Socha, J.; Pierzchalski, M.; Bałazy, R.; Ciesielski, M. Modelling top height growth and site index using repeated laser scanning data. *For. Ecol. Manag.* **2017**, *406*, 307–317. [[CrossRef](#)]

13. Wang, Y.; Matti, L.; Liang, X.; Jiri, P.; Antero, K.; Anttoni, J.; Liu, J.; Feng, Z. Is field-measured tree height as reliable as believed – A comparison study of tree height estimates from field measurement, airborne laser scanning and terrestrial laser scanning in a boreal forest. *ISPRS J. Photogramm.* **2019**, *147*, 132–145. [[CrossRef](#)]
14. Shao, T.; Qu, Y.; Du, J. A low-cost integrated sensor for measuring tree diameter at breast height (DBH). *Comput. Electron. Agric.* **2022**, *199*, 107140. [[CrossRef](#)]
15. Hao, Z.; Lin, L.; Post, C.J.; Jiang, Y.; Li, M.; Wei, N.; Yu, K.; Liu, J. Assessing tree height and density of a young forest using a consumer unmanned aerial vehicle (UAV). *New For.* **2021**, *52*, 843–862. [[CrossRef](#)]
16. Jin, C.; Oh, C.-y.; Shin, S.; Wilfred Njungwi, N.; Choi, C. A Comparative Study to Evaluate Accuracy on Canopy Height and Density Using UAV, ALS, and Fieldwork. *Forests* **2020**, *11*, 241. [[CrossRef](#)]
17. Chen, S.; Liang, D.; Ying, B.; Zhu, W.; Zhou, G.; Wang, Y. Assessment of an improved individual tree detection method based on local-maximum algorithm from unmanned aerial vehicle RGB imagery in overlapping canopy mountain forests. *Int. J. Remote Sens.* **2021**, *42*, 106–125. [[CrossRef](#)]
18. Stuart, K.; Tanja, G.M.S.; Jan-Peter, M.; Klaus, G. UAV-Based Photogrammetric Tree Height Measurement for Intensive Forest Monitoring. *Remote Sens.* **2019**, *11*, 758.
19. Mielcarek, M.; Stereńczak, K.; Khosravipour, A. Testing and evaluating different LiDAR-derived canopy height model generation methods for tree height estimation. *Int. J. Appl. Earth Obs. Geoinf.* **2018**, *71*, 132–143. [[CrossRef](#)]
20. Hao, J.; Chen, S.; Li, D.; Wang, C.; Ji, Y. Papaya Tree Detection with UAV Images Using a GPU-Accelerated Scale-Space Filtering Method. *Remote Sens.* **2017**, *9*, 721.
21. Guerra, H.J.; Cosenza, D.N.; Rodriguez, L.C.E.; Silva, M.; Tomé, M.; Díaz, V.R.A.; González, F.E. Comparison of ALS- and UAV(SfM)-derived high-density point clouds for individual tree detection in Eucalyptus plantations. *Int. J. Remote Sens.* **2018**, *39*, 5211–5235. [[CrossRef](#)]
22. Grigorijs, G.; Stefan, W.M.; Shaun, R.L.; Andrew, E. Efficiency of Individual Tree Detection Approaches Based on Light-Weight and Low-Cost UAS Imagery in Australian Savannas. *Remote Sens.* **2018**, *10*, 161.
23. Ramalho, D.; Lassiter, H.; Wilkinson, B.; Whitley, T.; Ifju, P.; Logan, S.; Peter, G.; Vogel, J.; Martin, T. Moving to Automated Tree Inventory: Comparison of UAS-Derived Lidar and Photogrammetric Data with Manual Ground Estimates. *Remote Sens.* **2020**, *13*, 72. [[CrossRef](#)]
24. Shimizu, K.; Nishizono, T.; Kitahara, F.; Fukumoto, K.; Saito, H. Integrating terrestrial laser scanning and unmanned aerial vehicle photogrammetry to estimate individual tree attributes in managed coniferous forests in Japan. *Int. J. Appl. Earth Obs.* **2022**, *106*, 102658. [[CrossRef](#)]
25. Yoshii, T.; Matsumura, N.; Lin, C. Integrating UAV-SfM and Airborne Lidar Point Cloud Data to Plantation Forest Feature Extraction. *Remote Sens.* **2022**, *14*, 1713. [[CrossRef](#)]
26. Corey, F.; Gregory, J.M.; Guillermo, C. Detection of Coniferous Seedlings in UAV Imagery. *Forests* **2018**, *9*, 432.
27. Hartley, R.J.L.; Leonardo, E.M.; Massam, P.; Watt, M.S.; Estarija, H.J.; Wright, L.; Melia, N.; Pearse, G.D. An Assessment of High-Density UAV Point Clouds for the Measurement of Young Forestry Trials. *Remote Sens.* **2020**, *12*, 4039. [[CrossRef](#)]
28. Stefano, P.; Bruce, T.; Rasmus, A. Tree-Stump Detection, Segmentation, Classification, and Measurement Using Unmanned Aerial Vehicle (UAV) Imagery. *Forests* **2018**, *9*, 102.
29. Stefano, P.; Svein, S.; Aksel, G. Use of UAV Photogrammetric Data for Estimation of Biophysical Properties in Forest Stands Under Regeneration. *Remote Sens.* **2019**, *11*, 233.
30. Julian, M.N.; David, M.N. Herbivores equalize the seedling height growth of three dominant tree species in an African tropical rain forest. *Forest Ecol. Manag.* **2013**, *310*, 555–566.
31. Zhang, W.; Qi, J.; Wan, P.; Wang, H.; Xie, D.; Wang, X.; Yan, G. An Easy-to-Use Airborne LiDAR Data Filtering Method Based on Cloth Simulation. *Remote Sens.* **2016**, *8*, 501. [[CrossRef](#)]
32. Zhou, X.; Wang, F.; Huang, H.; Feng, Z.; Xiao, X.; Li, Y. Number and Parameters Extraction of Tree Well Based on UAV Remote Sensing in Cutting Area. *Trans. Chin. Soc. Agric. Mach.* **2021**, *52*, 201–206.
33. Canny, J. A computational approach to edge detection. *IEEE Trans. Pattern Anal. Mach. Intell.* **1986**, *8*, 679–698. [[CrossRef](#)]
34. Zhuang, P.; Fu, X.; Huang, Y.; Ding, X. Image Enhancement Using Divide-and-Conquer Strategy. *J. Vis. Commun. Image R.* **2017**, *45*, 137–146. [[CrossRef](#)]
35. Xiangchu, F.; Liang, L.; Xixi, J.; Weiwei, W. A divide-and-conquer stochastic alterable direction image denoising method. *Signal Process.* **2015**, *108*, 90–101.
36. Gu, J.; Grybas, H.; Congalton, R.G. Individual Tree Crown Delineation from UAS Imagery Based on Region Growing and Growth Space Considerations. *Remote Sens.* **2020**, *12*, 2363. [[CrossRef](#)]
37. Chalmers, D.J.; Ende, B.V.D. Productivity of Peach Trees: Factors Affecting Dry-weight Distribution During Tree Growth. *Ann. Bot.* **1975**, *39*, 423–432. [[CrossRef](#)]
38. Jan, D.; Jyoteshwar, N.; Sebastian, H.; Carsten, T.; Reiner, Z.; Peter, N.B.; Timothy, A.M. Measurement of Within-Season Tree Height Growth in a Mixed Forest Stand Using UAV Imagery. *Forests* **2017**, *8*, 231.
39. Bourgoin, C.; Betbeder, J.; Couteron, P.; Blanc, L.; Dessard, H.; Oszwald, J.; Le Roux, R.; Cornu, G.; Reymondin, L.; Mazzei, L. UAV-based canopy textures assess changes in forest structure from long-term degradation. *Ecol. Indic.* **2020**, *115*, 106386. [[CrossRef](#)]

40. Ferreira, M.P.; de Almeida, D.R.A.; de Almeida Papa, D.; Minervino, J.B.S.; Veras, H.F.P.; Formighieri, A.; Santos, C.A.N.; Ferreira, M.A.D.; Figueiredo, E.O.; Ferreira, E.J.L. Individual tree detection and species classification of Amazonian palms using UAV images and deep learning. *For. Ecol. Manag.* **2020**, *475*, 118397.
41. Zarco-Tejada, P.J.; Diaz-Varela, R.; Angileri, V.; Loudjani, P. Tree height quantification using very high resolution imagery acquired from an unmanned aerial vehicle (UAV) and automatic 3D photo-reconstruction methods. *Eur. J. Agron.* **2014**, *55*, 89–99. [[CrossRef](#)]
42. Panagiotidis, D.; Abdollahnejad, A.; Surovy, M. Determining tree height and crown diameter from high-resolution UAV imagery. *Int. J. Remote Sens.* **2017**, *38*, 2392–2410. [[CrossRef](#)]
43. Goodbody, T.; White, J.; Coops, N.; LeBoeuf, A. Benchmarking acquisition parameters for digital aerial photogrammetric data for forest inventory applications: Impacts of image overlap and resolution. *Remote Sens. Environ.* **2021**, *265*, 112677. [[CrossRef](#)]
44. Wu, D.; Johansen, K.; Phinn, S.; Robson, A.; Tu, Y. Inter-comparison of remote sensing platforms for height estimation of mango and avocado tree crowns. *Int. J. Appl. Earth Obs.* **2020**, *89*, 102091. [[CrossRef](#)]
45. Stovall, A.; Shugart, H.; Yang, X. Tree height explains mortality risk during an intense drought. *Nat. Commun.* **2019**, *10*, 4385. [[CrossRef](#)]
46. Julian, T.; Martin, M.; Peter, S.; Alzbeta, G.; Jan, M. UAV RTK/PPK Method—An Optimal Solution for Mapping Inaccessible Forested Areas? *Remote Sens.* **2019**, *11*, 721.
47. Bertacchi, A. UAVs Technology as a Complementary Tool in Post-Fire Vegetation Recovery Surveys in Mediterranean Fire-Prone Forests. *Forests* **2022**, *13*, 1009. [[CrossRef](#)]
48. Krzysztof, S.; Milosz, M.; Bogdan, W.; Karol, B.; Grzegorz, Z.; Andrzej, M.J.; Wojciech, O.; Maciej, S. Factors influencing the accuracy of ground-based tree-height measurements for major European tree species. *J. Environ. Manag.* **2018**, *231*, 1284–1292.
49. Yu, H.T.; Kasper, J.; Stuart, P.; Andrew, R. Measuring Canopy Structure and Condition Using Multi-Spectral UAS Imagery in a Horticultural Environment. *Remote Sens.* **2019**, *11*, 269.
50. Ma, Q.; Su, Y.; Tao, S.; Guo, Q. Quantifying individual tree growth and tree competition using bi-temporal airborne laser scanning data: A case study in the Sierra Nevada Mountains, California. *Int. J. Digit. Earth* **2018**, *11*, 485–503. [[CrossRef](#)]
51. Ziliani, M.; Parkes, S.; Hoteit, I.; McCabe, M. Intra-Season Crop Height Variability at Commercial Farm Scales Using a Fixed-Wing UAV. *Remote Sens.* **2018**, *10*, 2007. [[CrossRef](#)]
52. Juan, G.; Eduardo, G.; Vicente, J.M.; Sonia, P.F.; Margarida, T.; Ramon, A.D. Use of Multi-Temporal UAV-Derived Imagery for Estimating Individual Tree Growth in *Pinus pinea* Stands. *Forests* **2017**, *8*, 300.
53. McDowell, N.G.; Allen, C.D.; AndersonTeixeira, K.; Aukema, B.H.; BondLamberty, B.; Chini, L.; Clark, J.S.; Dietze, M.; Grossiord, C.; HanburyBrown, A.; et al. Pervasive shifts in forest dynamics in a changing world. *Science* **2020**, *368*, 6494. [[CrossRef](#)] [[PubMed](#)]
54. Flurin, B.; Olivier, B.; Benjamin, P.; Valerie, T.; Martin, P.G.; David, C.F. Twentieth century redistribution in climatic drivers of global tree growth. *Sci. Adv.* **2019**, *5*, eaat4313.
55. Mizanur, R.; Mahmuda, I.; Aster, G.; Achim, B. Trends in tree growth and intrinsic water-use efficiency in the tropics under elevated CO₂ and climate change. *Trees* **2019**, *33*, 623–640.
56. Keiko, F.; Tetsuji, O.; Nobuya, M.; Shigejiro, Y.; Yukio, T. The effect of weeding frequency and timing on the height growth of young sugi (*Cryptomeria japonica*) in southwestern Japan. *J. For. Res.* **2017**, *22*, 1–4.

Disclaimer/Publisher’s Note: The statements, opinions and data contained in all publications are solely those of the individual author(s) and contributor(s) and not of MDPI and/or the editor(s). MDPI and/or the editor(s) disclaim responsibility for any injury to people or property resulting from any ideas, methods, instructions or products referred to in the content.